Anal. Chem. **2004,** *76,* 1−8

Accelerated Articles

Quantitative Submonolayer Spatial Mapping of Arg-Gly-Asp-Containing Peptide Organomercaptan Gradients on Gold with Matrix-Assisted Laser Desorption/Ionization Mass Spectrometry

Qian Wang, Jennifer A. Jakubowski, Jonathan V. Sweedler, and Paul W. Bohn*

Department of Chemistry and Beckman Institute for Advanced Science and Technology, University of Illinois at Urbana−Champaign, 600 South Mathews Avenue, Urbana, Illinois 61801

Peptides containing the tripeptide sequence Arg-Gly-Asp (RGD) have the ability to bind to members of the integrin superfamily of cell-surface receptors and direct cellular adhesion and haptotaxis. The goal of this work is the development of a rapid and effective method for the quantitative submonolayer spatial composition mapping of surfaces displaying molecular assemblies of RGD-containing organomercaptan peptides on a Au surface using matrix-assisted laser desorption/ionization time-of-flight mass spectrometry (MALDI-MS). Quantitation of the RGD peptide is achieved by determining the peak intensity of the protonated molecular ion, $(M + H)^+$, relative to the $(M + H)^+$ peak for an internal standard, which is similar chemically but with glutamic acid (E) substituted for aspartic acid (D). Using optimized sample preparation procedures, a bilinear calibration was obtained between the quantitative peak intensity ratio and the mole fraction of the RGD-containing peptide. Quantitative compositions were determined with relative standard deviations of $<10\%$, even in the presence of $10\times$ spot-to-spot variations in the absolute signal intensities, by using this internal standard approach. This MALDI-MS quantitative analysis method was employed to probe variable-width two-component counterpropagating electrochemically generated gradients of the two peptides, prepared by coupling in-plane electrochemical potential gradients with the electrosorption reactions of organothiols to vary the composition laterally. The measured lateral composition profiles match the quasi-linear potential gradient model and yield profiles that overlap to a high degree of fidelity in potential space. Thus, MALDI-MS spatial composition mapping should become a powerful tool for the preparation of designed surfaces facilitating the study of cellular adhesion and motility and cell−cell interactions.

Immobilizing proteins and peptides found in the extracellular matrix (ECM) on surfaces is a powerful method to probe the response of cells to their external environment, because cellular adhesion to the ECM influences the shape, growth, motility, and metabolism of cells.[1−3] It has been shown both theoretically and experimentally that gradients of cell receptor ligands are a directing force in cellular haptotaxis and that moderating the surface density of ECM proteins results in a variation of cell−substratum adhesion strength.[4] For example, the tripeptide sequence arginine-glycine-aspartic acid (RGD) is a common motif in adhesive ECM proteins, which is recognized by cell membrane receptors from the integrin superfamily.[5] Furthermore, substrates modified with the RGD-containing peptides by themselves are competent to support the adhesion and spreading of mammalian cells.[6,7] Griffith et al.[8] reported that cell migration speed increases

* To whom correspondence should be addressed. E-mail: bohn@scs.uiuc.edu.

(1) Ingber, D. E. *Proc. Natl. Acad. Sci. U.S.A.* **1990**, *87*, 3579−3583.
(2) Boudreau, N.; Sympson, C. J.; Werb, Z.; Bissell, M. J. *Science* **1995**, *267*, 891−893.
(3) Basson, C. T.; Kocher, O.; Basson, M. D.; Asis, A.; Madri, J. A. *J. Cell. Phys.* **1992**, *153*, 118−128.
(4) Maheshwari, G.; Wells, A.; Griffith, L. G.; Lauffenburger, D. A. *Biophys. J.* **1999**, *76*, 2814−2823.
(5) Ruoslahti, E.; Pierschbacher, M. D. *Science* **1987**, *238*, 491−497.
(6) Roberts, C.; Chen, C. S.; Mrksich, M.; Martichonok, V.; Ingber, D. E.; Whitesides, G. M. *J. Am. Chem. Soc.* **1998**, *120*, 6548−6555.
(7) Houseman, B. T.; Mrksich, M. *Biomaterials* **2001**, *22*, 943−955.
(8) Maheshwari, G.; Brown, G.; Lauffenburger, D. A.; Wells, A.; Griffith, L. G. *J. Cell Sci.* **2000**, *113*, 1677−1686.

10.1021/ac030335+ CCC: $27.50
Published on Web 11/27/2003

to a plateau with increasing RGD-containing peptide (YGRGD) density. However, most previous studies address the influence of spatially uniform distributions of RGD-containing peptides on cell−substratum interactions. Access to quantitatively characterized nonuniform RGD peptide distributions with controlled characteristics would be a significant boon to cell motility studies inasmuch as the spatial gradient of ligand density is known to affect cellular haptotaxis.

To this end, surfaces with well-defined nonuniform spatial composition profiles of RGD-containing tetradecapeptides on Au have been prepared.[9] Several methods have been demonstrated that use self-assembled monolayers (SAMs) to generate gradients in surface properties, including photoimmobilization of peptides on SAMs[10] and reaction cross-diffusion.[11,12] For example, R-phycoerythrin gradients have been created using a heterobifunctional photolinking agent with varying exposure time to laser irradiation.[13] Also, a microfluidic system has recently been used to generate surface and solution gradients of laminin in order to study neuronal growth.[14,15] In our laboratory, a new technique to make surface composition gradients on thin Au electrodes has been developed, which exploits the electrosorption properties of alkanethiols.[16−20] Adsorbed thiols on Au, RS−Au, are electrochemically stripped from Au surfaces by reductive desorption, which results in the release of RS.[21−24] By coupling the thiol-stripping reaction to a nonuniform in-plane electrochemical potential distribution, $V(x)$, thiols can be stripped from regions of the surface where the local potential favors desorption. The resulting gradient in surface potential produces a surface composition profile, $\Gamma(x)$, that progresses from bare Au on one end to full thiol coverage at the other end. The bare regions can then be back-filled with another thiol, creating a two-component full monolayer. Changing the terminal group, therefore, allows two-component systems with spatially graded chemical and physical properties to be fabricated. The spatial position of the transition region between the two components depends on the value of desorption peak potential, E^0_{des}, for the first thiol. Because the electrochemical strategy for creating two-component gradient structures is largely independent of the ω-functional group of the thiol, molecular recognition motifs may be inserted at the thiol terminus. For example, the RGD ligand for the integrin class of cell surface receptors can be inserted and thus used to effect directed cellular motion.

Because the details of cellular haptotaxis depend on the spatial rate of change of ECM ligands, $d\Gamma/dx$, it is important to characterize the spatial variation in the transition region in order to understand how the range and spatial dispersion of the in-plane RGD peptide composition distributions couple to cellular motility. Various approaches have been taken to characterizing nonbiologically active surface composition gradients. Contact angle measurement and surface plasmon reflectometry imaging have been used to map the wettability and resonance variation of alkanethiol gradients,[15,16] and atomic force microscopy and fluorescence microscopy of alkanethiol gradients have also been used.[17,18] In addition to these largely physical mapping approaches, molecular specificity has been achieved by surface-enhanced Raman spectroscopy (SERS) chemical mapping of aromatic thiol gradients.[19] However, SERS is not capable of providing molecularly specific information about intermediate molecular weight peptides. What is needed is a tool that is sensitive to submonolayer amounts and can characterize specific molecules with good spatial resolution.

Matrix-assisted laser desorption/ionization time-of-flight mass spectrometry (MALDI-MS) has been used extensively for the qualitative analysis of biological materials such as peptides and proteins.[25−29] MALDI-MS requires the use of an excess of a small-molecule matrix that serves to absorb energy from the laser and transfer it to the macromolecular analyte, resulting in the desorption of primarily intact, protonated molecular ions ($M + H^+$). This soft ionization technique can analyze samples up to 300 kDa, is very sensitive, with the detection limits in the attomole range, and can analyze spatially limited areas corresponding to the diameter of the focused laser beam. Based on its high sensitivity and low detection limit, MALDI-MS has been used to characterize small molecule self-assembled monolayers,[31−36] and Su and Mrksich have used MALDI-MS to monitor chemical

(9) Wang, Q.; Bohn, P. W. *J. Phys. Chem. B*, in press.
(10) Herbert, C. B.; McLernon, T. L.; Hypolite, C. L.; Adams, D. N.; Pikus, L.; Huang, C. C.; Fields, G. B.; Letourneau, P. C.; Distefano, M. D.; Hu, W. S. *Chem. Biol.* **1997**, *4*, 731−737.
(11) Liedberg, B.; Tengvall, P. *Langmuir* **1995**, *11*, 3821−3827.
(12) Liedberg, B.; Wirde, M.; Tao, Y. T.; Tengvall, P.; Gelius, U. *Langmuir* **1997**, *13*, 5329−5334.
(13) Hypolite, C. L.; McLernon, T. L.; Adams, D. N.; Chapman, K. E.; Herbert, C. B.; Huang, C. C.; Distefano, M. D.; Hu, W. S. *Bioconjugate Chem.* **1997**, *8*, 658−663.
(14) Jeon, N. L.; Dertinger, S. K. W.; Chiu, D. T.; Choi, I. S.; Stroock, A. D.; Whitesides, G. M. *Langmuir* **2000**, *16*, 8311−8316.
(15) Dertinger, S. K. W.; Jiang, X. Y.; Li, Z. Y.; Murthy, V. N.; Whitesides, G. M. *Proc. Natl. Acad. Sci. U.S.A.* **2002**, *99*, 12542−12547.
(16) Terrill, R. H.; Balss, K. M.; Zhang, Y. M.; Bohn, P. W. *J. Am. Chem. Soc.* **2000**, *122*, 988−989.
(17) Balss, K. M.; Coleman, B. D.; Lansford, C. H.; Haasch, R. T.; Bohn, P. W. *J. Phys. Chem. B* **2001**, *105*, 8970−8978.
(18) Plummer, S. T.; Bohn, P. W. *Langmuir* **2002**, *18*, 4142−4149.
(19) Balss, K. M.; Fried, G. A.; Bohn, P. W. *J. Electrochem. Soc.* **2002**, *149*, C450−C455.
(20) Balss, K. M.; Kuo, T. C. B., P. W. *J. Phys. Chem. B* **2003**, *107*, 994−1000.
(21) Widrig, C. A.; Chung, C.; Porter, M. D. *J. Electroanal. Chem.* **1991**, *310*, 335−359.
(22) Walczak, M. M.; Popenoe, D. D.; Deinhammer, R. S.; Lamp, B. D.; Chung, C. K.; Porter, M. D. *Langmuir* **1991**, *7*, 2687−2693.
(23) Weisshaar, D. E.; Lamp, B. D.; Porter, M. D. *J. Am. Chem. Soc.* **1992**, *114*, 5860−5862.
(24) Hobara, D.; Miyake, O.; Imabayashi, S.; Niki, K.; Kakiuchi, T. *Langmuir* **1998**, *14*, 3590−3596.
(25) Stump, M. J.; Fleming, R. C.; Gong, W. H.; Jaber, A. J.; Jones, J. J.; Surber, C. W.; Wilkins, C. L. *Appl. Spectrosc. Rev.* **2002**, *37*, 275−303.
(26) Kruse, R. A.; Rubakhin, S. S.; Romanova, E. V.; Bohn, P. W.; Sweedler, J. V. *J. Mass Spectrom.* **2001**, *36*, 1317−1322.
(27) Page, J. S.; Sweedler, J. V. *Anal. Chem.* **2002**, *74*, 6200−6204.
(28) Zhang, L.; Orlando, R. *Anal. Chem.* **1999**, *71*, 4753−4757.
(29) Neubert, H.; Jacoby, E. S.; Bansal, S. S.; Iles, R. K.; Cowan, D. A.; Kicman, A. T. *Anal. Chem.* **2002**, *74*, 3677−3683.
(30) Walker, A. K.; Land, C. M.; Kinsel, G. R.; Nelson, K. D. *J. Am. Soc. Mass Spectrom.* **2000**, *11*, 62−68.
(31) Brockman, A. H.; Dodd, B. S.; Orlando, N. *Anal. Chem.* **1997**, *69*, 4716−4720.
(32) Jordan, R.; West, N.; Ulman, A.; Chou, Y. M.; Nuyken, O. *Macromolecules* **2001**, *34*, 1606−1611.
(33) Fukuo, T.; Monjushiro, H.; Hong, H. G.; Haga, M. A.; Arakawa, R. *Rapid Commun. Mass Spectrom.* **2000**, *14*, 1301−1306.
(34) Haga, H.; Hong, H. G.; Shiozawa, Y.; Kawata, Y.; Monjushiro, H.; Fukuo, T.; Arakawa, R. *Inorg. Chem.* **2000**, *39*, 4566−4573.
(35) Janshoff, A.; Steinem, C.; Michalke, A.; Henke, C.; Galla, H. J. *Sens. Actuator, B: Chem.* **2000**, *70*, 243−253.
(36) Cao, Y. H.; Li, Y. S.; Tseng, J. L.; Desiderio, D. M. *Spectroc. Acta Pt. A: Mol. Biomol. Spectrosc.* **2001**, *57*, 27−34.

reactions of alkanethiol SAMs.[37] MALDI-MS also appears to be ideal for the study of surface-binding proteins, because it requires little sample preparation, such that the addition of a drop of matrix solution to the protein-coated surface prepares the sample for mass spectrometric analysis. However, quantitation of proteins and peptides by MALDI-MS is difficult, because the absolute intensities of the detected ions depend on their chemical nature and the inhomogeneous distribution of analytes within the matrix, which together cause poor shot-to-shot and sample-to-sample reproducibility. To overcome this problem, internal standards with similar chemical structures are added to the sample and the intensity ratio of the internal standard to the analyte is used for quantitation.[38−41] In the present work, we combine high-sensitivity MALDI-MS sampling with an internal peptide standard and high spatial resolution to achieve quantitative submonolayer spatial mapping of RGD-containing peptide gradients.

Sample preparation for MALDI-MS is a critical step that greatly affects the quality of the MALDI mass spectra obtained.[42] There are many factors in sample preparation that influence the crystallization of samples, including selection of matrix, composition of solvent, and matrix-to-analyte ratio. The present investigation addresses the quantitation of SAMs of the RGD-containing peptide **I** on a gold surface by MALDI-MS, using peptide **II**, in which aspartic acid (D) is substituted by glutamic acid (E) as the internal standard. We have optimized the deposition method and concentration of matrix, yielding quantitative determinations of the target peptide, **I**. Biologically active gradients of peptide **I** are fabricated electrochemically in the presence of peptide **II**, the nonbinding peptide, and MALDI-MS quantitative analysis is applied to map the spatial distribution of these gradient components.

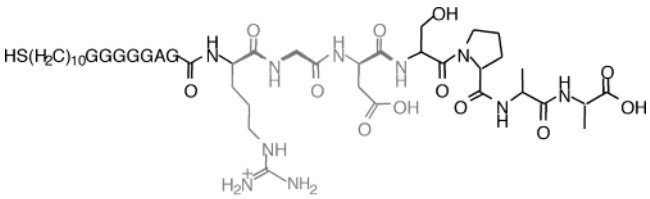

I

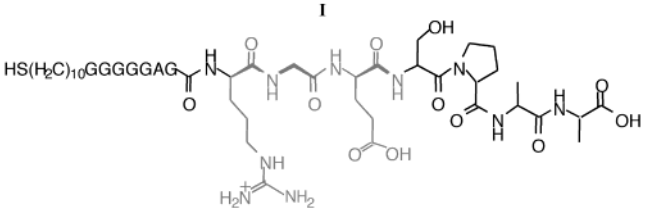

II

EXPERIMENTAL SECTION

Materials. The linear version of the RGD-containing thiol, **I**, and RGE-containing thiol, **II**, were synthesized by coupling mercaptoundecanoic acid to the amine terminal of the tetradecapeptide, GGGGGAGRGDSPAA for **I** and GGGGGAGRGESPAA for **II**, at the University of Illinois at Urbana−Champaign Biotechnology Center. Products were characterized mass spectrometrically with $M + H^+$ of 1286.8 Da for **I** and 1301.0 Da for **II**. The matrix chemical 2,5-dihydroxybenzoic acid (DHB) was purchased from ICN Biomedical. Sinapinic acid (3,5-dimethoxy-4-hydroxycinnamic acid) (SA), trifluoroacetic acid (TFA), and bovine insulin were purchased from Sigma, and α-cyano-4-hydroxycinnamic acid (CCA) was purchased from Aldrich. KOH, Optima grade methanol (MeOH), acetone, acetonitrile, and 2-propanol were purchased from Fisher Scientific. Absolute ethanol (EtOH) was purchased from Aaper Alcohol and Chemical Co. Acidic peptide and α-bag cell peptide were obtained from American Peptide Co. (Sunnyvale, CA). Water used to prepare the matrixes was obtained from Burdick and Jackson (Muskegon, MI). All reagents were used as received.

Substrate Preparation. Substrates for Au deposition were single-polished silicon (100) wafers. Prior to metal deposition, wafers were cut into 3 × 1 cm pieces and cleaned in a freshly prepared Piranha solution (4:1 H_2SO_4/H_2O_2. *Caution: Piranha is a vigorous oxidant and should be used with extreme caution*!), rinsed thoroughly with doubly deionized H_2O and 2-propanol, and blown dry with N_2. The samples were then immediately transferred to the evaporation chamber. Chromium (1 nm) was evaporated to promote adhesion of Au on silicon substrates, followed by evaporation of 50 nm of Au. Samples were stored under N_2 until ready for use.

SAM Sample Preparation. Mixed monolayers of peptides **I** and **II** were prepared by immersing 1 × 1 cm Au films in a solution of **I** and **II** (total peptide concentration 20 μM; different composition ratios) in 1:1 EtOH/H_2O for 24 h. Samples were then removed from the solution, rinsed with deionized water and EtOH, and blown dry with N_2.

Gradient Formation. SAMs of **I** were prepared by immersing 3 × 1 cm Au film in 20 μM **I** in 1:1 EtOH/H_2O for 24 h. A bipotentiostat (Pine Instruments) employing a Ag/AgCl reference electrode and a Pt mesh counter electrode was used to apply the desired electrochemical potentials to the two ends of the working electrode in deaerated 0.25 M KOH/MeOH. Typically, SAMs of **I** were electrolyzed for 30 min, to achieve one-component gradients. After electrolysis, samples were quickly removed from the electrolyte solution, rinsed with MeOH, and reimmersed in a solution of a second thiol **II** for 1min to form the two-component gradients.

MALDI-MS Sample Preparation. The Au films with full monolayers or gradients were taped on a 45 × 45 mm stainless steel plate and carefully smoothed to remove entrapped air bubbles. For most experiments, matrix solution was pipetted directly onto the Au surface and allowed to air-dry. Droplets were generally 1.0 μL in volume. DHB was prepared in an 85% acetone, 15% water, and 0.3% trifluoroacetic acid. Solutions of SA and CCA (20 mg/mL) were prepared in 60% acetonitrile, 40% water, and 0.3% TFA. Then the samples were analyzed by MALDI-MS. The optical images of the MALDI matrixes were obtained by dark-field microscopy with an inverted Olympus IX70 microscope equipped with an Olympus DP12 microscope digital camera. A 10× microscope objective was employed in all cases.

(37) Su, J.; Mrksich, M. *Langmuir* **2003**, *19*, 4867−4870.
(38) Hensel, R. R.; King, R. C.; Owens, K. G. *Rapid Commun. Mass Spectrom.* **1997**, *11*, 1785−1793.
(39) Mirgorodskaya, O. A.; Kozmin, Y. P.; Titov, M. I.; Korner, R.; Sonksen, C. P.; Roepstorff, P. *Rapid Commun. Mass Spectrom.* **2000**, *14*, 1226−1232.
(40) Kang, M. J.; Tholey, A.; Heinzle, E. *Rapid Commun. Mass Spectrom.* **2000**, *14*, 1972−1978.
(41) Zhang, J.; Kinsel, G. R. *Langmuir* **2002**, *18*, 4444−4448.
(42) Cohen, S. L.; Chait, B. *Anal. Chem.* **1996**, *68*, 31−37.

Table 1. Test of Various Matrixes for Peptides **I** and **II**

matrix	**I**[a]	**II**[a]	intensity ratio (**I**/**II**)	RSD (%) ($n = 5$)	rel signal strength[b] (%)
2,5-dihydroxybenzoic acid (DHB)	G	G	1.424 ± 0.11	7.72	100
sinapinic acid (SA)	W	W	1.866 ± 0.13	6.97	40
α-cyano-4-hydroxy-cinnamic acid (CCA)	B	B	1.302 ± 0.16	12.3	28.6

[a] G, clear spectrum of MH^+ ion, reproducible; W, peaks detectable, but not adequate for quantitation due to weak signal; B, peaks detectable, but not adequate for quantitation due to interference from matrix peaks. [b] Signal strength, the fraction of spots where the signal-to-noise ratio exceeds a predetermined value.

Table 2. Deposition of DHB solution on sample surface

technique	**I**[a]	**II**[a]
electrospray	n/d	n/d[b]
spin-coating	B	B
dropping	G	G

[a] G, clear spectrum of MH^+ ion, reproducible; B, peaks detectable, but not adequate for quantitation due to interference from matrix peaks. [b] n/d, compounds not detected.

Spin-Coating Deposition. Spin-coating was achieved by depositing 100 μL of DHB solution onto the Au sample surface immediately before spinning at 4000 rpm for 40 s.

Electrospray Deposition. The sample plate was placed on an $x-y-z$ stage driven by three Newport motion actuators (Newport Corp., Irvine, CA) controlled by a computer through LabView software (National Instruments, Austin, TX). The outlet tip was constructed by incorporating a ground wire and an electrospray capillary (50-μm i.d./150-μm o.d., Polymicro Technologies) in a side-by-side configuration. This capillary delivered a solution to the tip containing 20 mg/mL DHB solution from a Harvard Apparatus syringe pump (South Natick, MA). Droplets eluted from the capillary and distributed matrix on the target.

MALDI Mass Spectrometry. The samples were mass profiled using a Voyager DE STR time-of-flight mass spectrometer with delayed ion extraction (Applied Biosystems). Mass spectra were obtained with a nitrogen laser (337 nm) as the desorption/ionization source. The instrument was used in linear mode with an acceleration voltage of 20 kV and a delayed extraction of 350 ns. The grid and guide wire voltages were set at 95 and 0.1% of the acceleration voltage, respectively. The mass spectra acquired were the average of 200 laser shots of ~100-μm diameter. Prior to sample analysis, an external mass calibration was performed using a peptide standard containing 60 pmol/μL α-bag cell peptide, 120 pmol/μL acidic peptide, and 120 pmol/μL bovine insulin. Signal intensity is reported as the apex of the mass spectral peak minus the baseline intensity.

RESULTS AND DISCUSSION

Matrix Selection. The effectiveness of MALDI matrixes is sample-dependent, such that no matrix is universal for all applications. In addition, the gradient surfaces of interest in these studies present special challenges in identifying the proper MALDI conditions, above and beyond the sensitivity issues associated with quantitative submonolayer mapping. In a typical MALDI sample preparation, the analyte is distributed throughout the matrix, while the analyte is fixed to the substrate and cannot be distributed throughout the matrix for these experiments. Additionally, the spatially varying substrate surface energy presents a challenge, because the spatially varying hydrophobic−hydrophilic character strongly influences matrix crystallization, which, in turn, greatly influences the quality of the MALDI spectrum.

To optimize the signal for the RGD samples, three common matrixes, DHB, SA, and CCA were examined. Table 1 shows the qualitative response characteristics of the three matrixes. To demonstrate the influence of matrix on signal, signal strength is defined as the fraction of laser spots where the signal-to-noise ratio (S/N) exceeds a specific threshold value. Examining the signal strength in this way for each matrix is important, because the S/N must be large enough to yield statistically reliable signals and to minimize potential inaccuracies originating from instrumental factors, such as analog-to-digital conversion. Among the matrixes tested, DHB gives the best results for both analytes **I** and **II,** allowing $(M + H)^+$ ions to be detected without interference from matrix ion peaks. SA produces signals sufficient for **I** and **II** to be detected; however, low absolute intensities result in lower S/N. CCA is not a good matrix for this application due to excessive interference by matrix peaks.

Optimization of Matrix Deposition. Various factors influence the quality of spectra, such as matrix molecule, matrix crystallization, and sample preparation procedures. Matrix crystallization influences MALDI mass spectra significantly, since poor crystallization can result in inefficient ionization of peptides. Several techniques, including spin-coating, electrospraying, and simply pipetting, were used to deposit the matrix on the sample, resulting in matrix crystallization as shown in Figure 1. Table 2 summarizes the qualitative characteristics of MALDI mass spectra obtained with each deposition method. Spin-coating produces matrixes with small, poorly defined crystals. Therefore, it is expected that the signal-to-noise ratio will be compromised due to poor energy transfer and ionization of analytes. Thick matrix layers are observed when the matrix is electrosprayed; however, they are poorly crystallized, as shown in Figure 1b. Analyte mass spectral signatures cannot be detected in these samples. In contrast, large, needlelike crystals of DHB are obtained by simply pipetting 1.0 μL of DHB solution on the sample surface, demonstrating excellent crystallization. Both analytes are reproducibly detected with high signal-to-noise ratio and minimal interference from matrix peaks when the DHB matrix is prepared in this manner. Thus, all further experiments are implemented with pipetted DHB matrix.

Optimization of Matrix Deposition Solution. It has been shown that the choice of matrix and deposition method is very important to the acquisition of high-quality mass spectra. Having identified the best matrix molecule and method of deposition, it is important to explore how the concentration of the matrix deposition solution affects the MALDI mass spectra. Figure 2 shows the effect of the concentration of matrix deposition solution on absolute signal strength and signal variance in a series of experiments in which the volume deposited was kept at 1.0 μL each time. Optimum signal strength is obtained at DHB concentrations in the range 40 mg/mL < [DHB] < 100 mg/mL, and

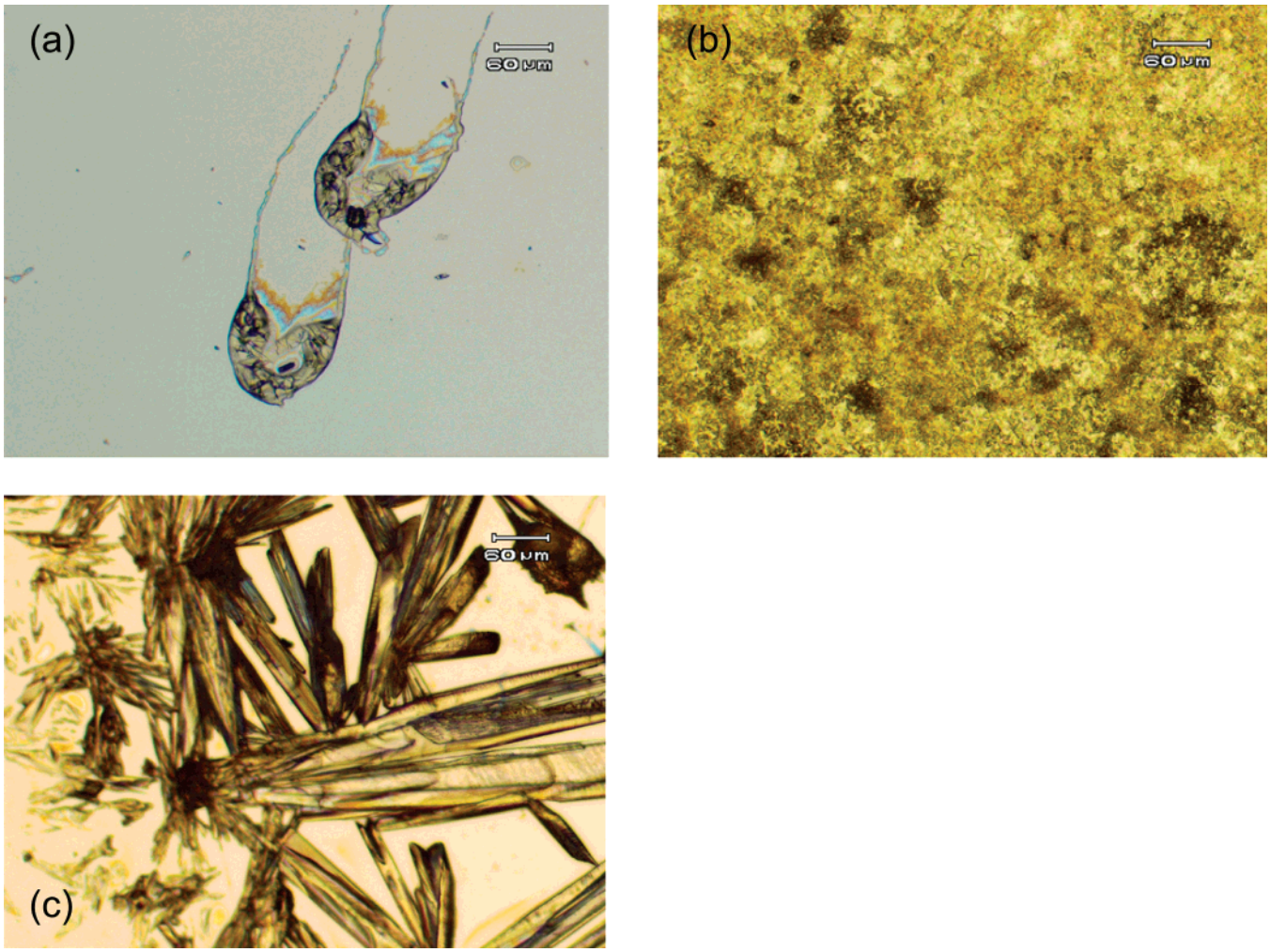

Figure 1. Optical images of 40 mg/mL DHB solution deposited on mixed monolayers of **I** and **II** by different techniques: (a) spin coating, (b) electrospray, (c) pipetting. The scale bar in each image is 60 μm.

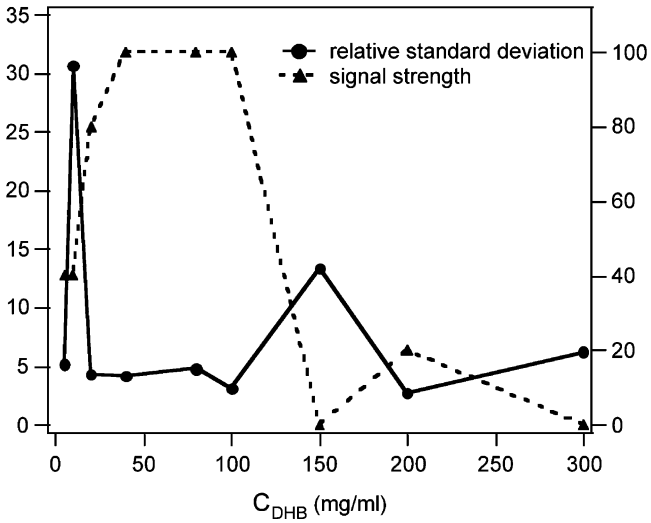

Figure 2. Relative standard deviation (closed circle, solid line−left ordinate) and signal strength (closed triangle, dashed line−right ordinate) as a function of DHB concentration.

the lowest relative standard deviation (RSD) ($n = 5$) is obtained in the range 20 mg/mL < [DHB] < 100 mg/mL. Acceptable sample variance is also achieved at DHB concentrations of 5 and 200 mg/mL, but the signal strength is relatively weak under these conditions. Optical microscopy of the SAM/matrix composites (not shown) prepared with different matrix concentrations shows poor crystallization of the matrix at both low and high concentrations. The DHB crystals are small and not well-formed at deposition solution concentrations below 20 mg/mL and are too thick to allow effective desorption of analytes when prepared from solutions with concentrations higher than 100 mg/mL. The optimum matrix concentration range is, therefore, 40−100 mg/mL DHB, and 40 mg/mL solutions were used for all further experiments.

Quantitative Analysis. Quantitation to determine the fractional surface coverage was achieved by using an internal standard, peptide **II**, which has one more methylene group (CH_2) than peptide **I**. All MALDI-MS mass spectral data for mixed monolayers were analyzed by calculating the ratio of intensities arising from the molecular ions of peptides **I** and **II**, $(M + H)_{\mathbf{I}}^+/(M + H)_{\mathbf{II}}^+$, as a function of the compositional fraction of peptide **I** in the mixed monolayer-formation solution, as shown in Figure 3. Seven locations on each sample were profiled. The lowest and highest were discarded, and the remaining five intensities were used to calculate relative intensities and standard deviations. Each point was determined by the average of the five intensities, with error bars indicating one standard deviation. As

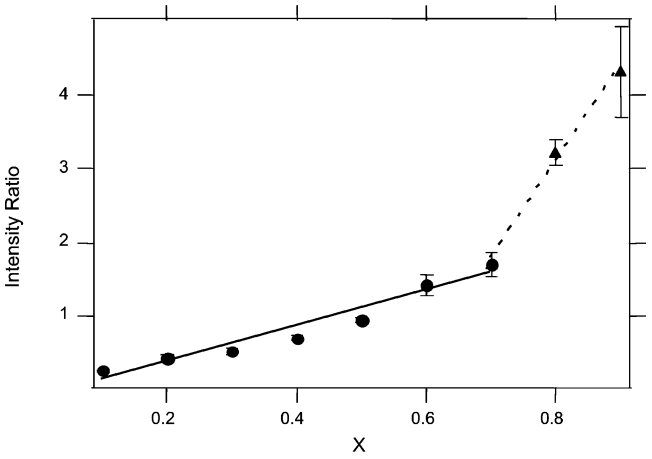

Figure 3. Intensity ratio for molecular ions corresponding to species **I** and **II**, $(M + H)_I/(M + H)_{II}$, as a function of the mole fraction of **I** in the mixed solution used to generate the mixed monolayers. The solid and dashed lines correspond to two linear fits with $y = -0.12 + 2.42x$ ($r^2 = 0.9718$) and $y = -7.45 + 13.2x$ ($r^2 = 0.9955$) corresponding to the mole fraction ranges, $0.1 < X < 0.7$ and $0.7 < X < 0.9$, respectively.

is often encountered with SAMs prepared from binary adsorbate solutions, the composition response is not a simple linear function of the mole fraction of **I** in the SAM formation solution. Instead, the response is fit by two linear regions in the range of peptide **I** fraction $0.1 < X < 0.7$ and $0.7 < X < 0.9$. The data are also well-described by a second-order polynomial, but this does not improve the fitting of the gradient composition profiles, vide infra, so the bilinear fit is used to describe the intensity ratio−mole fraction relationship. The standard deviations obtain in the range $0.1 < X < 0.8$ are all <10%. The relatively large standard deviation as $X_{RGD} = 0.9$ was caused by the weak signal of peptide **II** due to its low concentration. The small relative standard deviations indicate the great reproducibility obtained with this internal standard strategy to determine quantitative peptide compositions on SAMs. It is important to emphasize that the absolute signal intensities on a uniform composition sample vary from spot to spot by ∼10× for both **I** and **II**, so without the internal standard, quantitative compositional mapping by MALDI-MS is not possible. By introducing in the internal standard, a mass detection limit of 4.9×10^8 peptide molecules per laser spot was acquired.

Peptide Gradient Characterization by MALDI-MS. Substrates modified with RGD-containing peptides can support the adhesion and spreading of mammalian cells.[6,7] Because peptide **I** contains the cell recognition RGD sequence, and peptide **II** contains the RGE sequence, which does not support cell adhesion, these two peptides can be used to generate surface composition gradients on which the specific cellular activity, i.e., adhesion or motility, varies laterally. Since quantitative analysis of peptide **I** SAMs using peptide **II** as an internal standard is possible, the strategy was applied for chemical mapping of the **I**−**II** gradients.

MALDI-MS spectra of **I**−**II** gradients were achieved as a function of spatial position. Remembering that spatial position and applied potential are mapped onto each other in a one-to-one fashion in these linear gradients, Figure 4 shows the mass spectra obtained from a two-component gradient of peptides **I** and **II** prepared with an applied potential window from −1100 to −1400 mV versus Ag/AgCl. The spectra are labeled with the potential

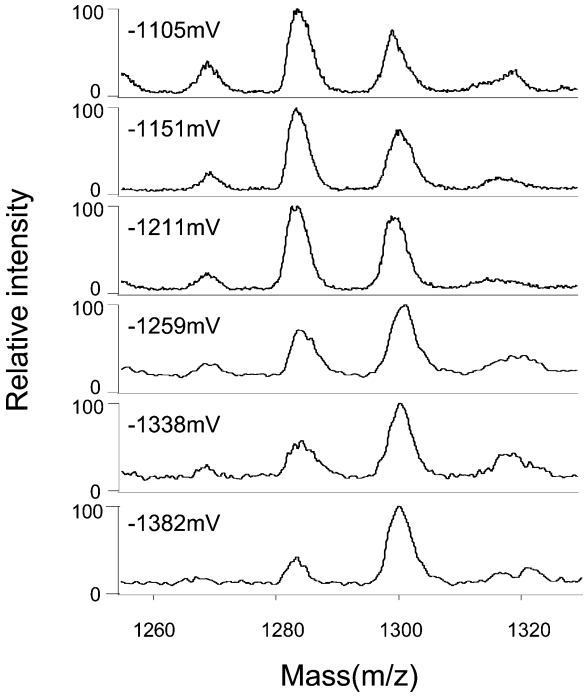

Figure 4. MALDI mass spectra for different spatial locations obtained from a **I**−**II** gradient sample produced between −1100 and −1400 mV. Each spectrum is labeled with a voltage corresponding to its linear position along the gradient. More positive potentials correspond to the end of the gradient with a larger fraction of peptide **I**. Matrix, 40 mg/mL DHB.

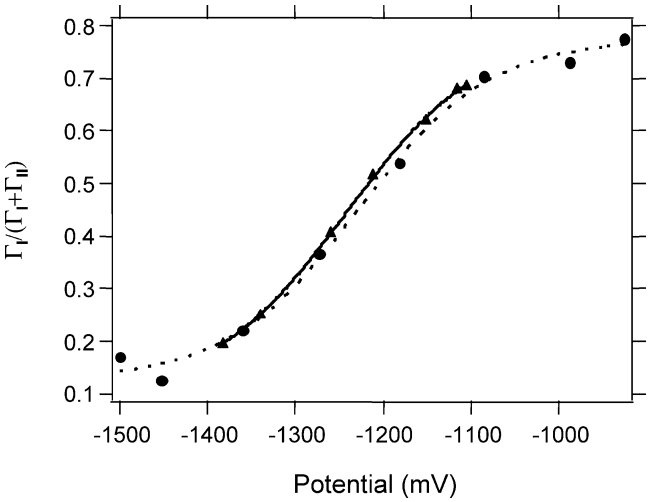

Figure 5. Composition profiles determined from the molecular ion intensity ratios as a function of applied potential (position) for two separate gradients of peptides **I** and **II**. Applied potential windows used to create the two gradients: −1100 to −1400 mV (solid line, closed triangles); −900 to −1500 mV (dashed line, closed circles).

corresponding to the spatial location from which they were acquired. Obviously the peak at $m/z = 1286$, due to **I**, increases, and that at $m/z = 1300$, due to **II**, decreases in intensity as the local potential, $V(x)$, shifts to more positive values, i.e., toward end of the gradient with pure **I**. The fraction of **I** on the surface, $\Gamma_I/(\Gamma_I + \Gamma_{II})$, as a function of applied potential (position) for two separate gradients is shown in Figure 5. $\Gamma_I/(\Gamma_I + \Gamma_{II})$ was extracted from the MALDI mass spectral molecular ion intensity ratios using the calibration shown in Figure 3. The transition region is characterized by fitting $\Gamma = \Gamma_I/(\Gamma_I + \Gamma_{II})$ as a function

of applied potential to a sigmoidal function of the form,

$$\Gamma(l) = \Gamma_b + (\Gamma_{max}/(1 + e^{(l_0 - l)/r})) \quad (1)$$

where Γ_b is the base fraction, Γ_{max} is the normalized maximum fraction, l_0 is the inflection point of the slope region, and r is a spatial rate constant related to the slope. The width of the gradient, W, is determined from the full width at half-maximum of the derivative of the fit function, $\Gamma(l)$. The l_0 and W values can be converted from potential space to physical space values using the magnitude of the applied potential window, ΔV, and the total length of the film.

The gradient formation characteristics are determined by the distribution of the local electrochemical potential, $V(x)$. By varying the width of the potential window, ΔV, experimentally one can learn how the gradient formation characteristics change as the local potential, $V(x)$, is moved relative to the physical frame of the active region. When ΔV decreases while keeping the length of the gradient constant, the potential drop per unit length, dV/dx, decreases, meaning that the transition region occupies a larger physical area of the film, although its width in potential space is unchanged. These interpretations are supported by the data for the second gradient shown in Figure 5, formed with an applied potential window -900 mV $> V(x) > -1500$ mV. It is apparent that the transition region does not change significantly in potential space; the gradient center and width keep relatively constant at -1228 and 261 mV, respectively, for the $\Delta V = 600$ mV potential window and -1242 and 275 mV for the $\Delta V = 300$ mV potential window. However, the gradient becomes wider in physical space as the gradient width increases from 11.7 to 24.6 mm when ΔV decreases from 600 to 300 mV. These observations are consistent with the predictions of the quasi-linear potential gradient model. The ability to control the spatial rate of change of the integrin ligand density is a critical requirement for the use of these biomaterials in cell motility studies and assays.

Although DHB is the optimum matrix for these experiments as revealed in Table 1, it is possible to acquire quantitative composition profiles from other matrixes. Figure 6 shows the intensity ratio for molecular ion peaks from peptides **I** and **II** as a function of applied potential (position) for two gradients prepared under the same conditions used to prepare the gradients characterized in Figure 5 using different matrixes. Even though the smaller signals obtained from the sinapinic acid matrix naturally lead to larger uncertainty in the measured intensity ratio, $(M + H)_{\mathbf{I}}^+/(M + H)_{\mathbf{II}}^+$, the gradient profiles are clearly consistent with the linear potential gradient model. Thus, the method of quantitative submonolayer spatial composition mapping by MALDI-MS is robust enough to generate good recovered profiles even with nonoptimal matrix conditions.

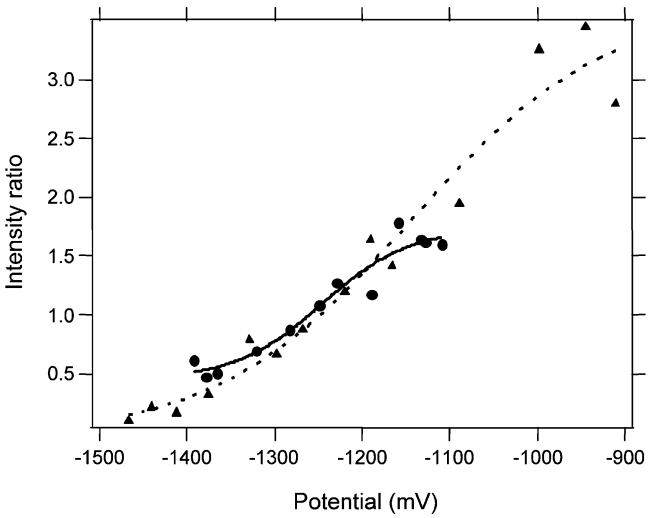

Figure 6. Intensity ratio for molecular ions corresponding to species **I** and **II**, $(M + H)_{\mathbf{I}}^+/(M + H)_{\mathbf{II}}^+$ as a function of applied potential for two separate gradients of peptides **I** and **II**. Applied potential window: -1100 to -1400 mV (solid line with closed circles); -900 to -1500mV (dashed line with closed triangles). Matrix, 20 mg/mL sinapinic acid. The ordinate is plotted as intensity ratio, because the performance of sinapinic acid relative to DHB did not support a full calibration.

CONCLUSIONS

Quantitative determinations of spatially varying surface composition of peptide SAMs by MALDI-MS was developed by using an internal standard with chemical properties similar to those of the analyte. The high sensitivity of MALDI-MS allows the detection of these low-coverage peptide monolayers down to coverages below 20% of a monolayer. The addition of an internal standard corrects for the spot-to-spot variation in absolute signal intensities and allows quantitative composition profiles to be recovered, with excellent spot-to-spot and sample-to-sample reproducibility. Details of the crystallization of the matrix, which is strongly influenced by the deposition method and the concentration of matrix, are critical to the quantitative analysis of peptide SAMs. After optimizing the sample preparation conditions, a calibration plot between signal ratio and composition of the SAM deposition solution was fit to two linear responses covering the ranges in the fractional composition of peptide **I**, $0.1 < X < 0.7$ and $0.7 < X < 0.9$. The ability to guide the small laser spot (100 μm) using MALDI-MS provides the ability to probe the composition profiles of the two-component counterpropagating composition gradients of peptide **I**, containing cell recognition sequence RGD, and the protein adhesion-resistant peptide **II**.

Spatial composition profiles mapped by MALDI-MS are well-described by a sigmoidal function, from which the center potential and transition region width could be determined. The gradient center is found to shift in physical space, but not in potential space, and the rate of compositional change, $d\Gamma/dx$, in the transition region is easily controlled when the width of the applied potential window, ΔV, is changed. These results are consistent with the quasi-linear potential gradient model. One could imagine extending these results by pairing this internal standard approach with the new technique of imaging mass spectrometry, where a laser spot is scanned across the sample and spatial maps of peptide distributions reconstructed.[43−46] Spatial distributions of multiple peptides would then be measurable, yielding unmatched qualitative and quantitative information. The achievement of tunable composition gradients of RGD-containing ligands for the integrin

(43) Kruse, R.; Sweedler, J. V. *J. Am. Soc. Mass Spectrom.* **2003**, *14*, 752−759.
(44) Spengler, B.; Hubert, M. *J. Am. Soc. Mass Spectrom.* **2002**, *13*, 735−748.
(45) Stoeckli, M.; Chaurand, P.; Hallahan, D. E.; Caprioli, R. M. *Nat. Med.* **2001**, *7*, 493−496.
(46) Todd, P. J.; Schaaff, T. G.; Chaurand, P.; Caprioli, R. M. *J. Mass Spectrom.* **2001**, *36*, 355−369.

superfamily of heterodimeric membrane receptors has important implications for the study of cellular motility and haptotactic behavior. The ability to evaluate such peptide gradients accurately will enable the effect of complex peptide distributions on cellular haptotaxis to be better understood.

ACKNOWLEDGMENT

This work was supported by grants from the National Institutes of Health (NIGMS GC10825, the Cell Migration Consortium, and NS31609) and the National Science Foundation (CHE 99-10236). The authors thank Dr. Donald M. Cannon, Jr. and Cory Scanlan for help with the spin-coating and the electrospray deposition of MALDI matrix.

Received for review September 22, 2003. Accepted November 3, 2003.

AC030335+